Proceedings of the
47th IEEE Conference on Decision and Control
Cancun, Mexico, Dec. 9-11, 2008

Continuous Rolling Motion Control for the Acrobot Composed of Rounded Links

Shimpei Isobe, Shigeki Nakaura and Mitsuji Sampei
Tokyo Institute of Technology

Abstract— **This paper describes the modeling of the Acrobot composed of 2 links with a curved contour and the continuous rolling motion control for this Acrobot. The outer contour of each link is shaped from the arc whose radius is different by the tip and the sidepiece of the link. The model differs according to the contact point between the Acrobot and the ground. Therefore, it is difficult to control the whole motion via common control strategy. From an intuitive analysis based on the Acrobot's energy while the Acrobot rolls with a certain constant relative angle, control strategy is constructed in two phases. The phases are when the Acrobot rolls with lowering(downward phase) and raising(upward phase) the center of the gravity. As the control in upward phase needs to lower the COG of the Acrobot, a collision between the Acrobot and the ground becomes unavoidable. Therefore, analysis of this collision phenomenon is also conducted. At last, by selecting the output functions that can achieve the control objective at each phase and applying Output Zeroing control, continuous rolling motion is realized in numerical simulation.**

I. Introduction

The Acrobot is two-link underactuated robot. Because the Acrobot is underactuated, it is very interesting from the nonlinear control point of view. Therefore, there are many researches about motion control of the Acrobot. For example, swing up control problem[1][2] which is the most famous problem, and hopping gait control problem[3] are dealt with in past researches.

The purpose of this paper is to achieve continuous rolling motion for the Acrobot shown in Fig. 1. Nakakuki et al. realized rolling motion with three links serial robot in numerical simulation and experiment[4][5]. Because the Acrobot has less input than Nakakuki's system, it is more difficult problem. Furthermore, to realize rolling motion of the Acrobot, we need to deal with rolling constraint and switching of models. Therefore we think there is a room for the further research about the Acrobot.

This paper is organized as follows. In Section II, a model of the Acrobot to realize rolling motion is explained. First, we explain a structure of the link of the Acrobot. Next, we explain models to realize rolling motion and derive dynamic equation. In Section III, intuitive analysis and control of rolling motion is explained. First, we divide the rolling motion into three phases and analyze the energy of the Acrobot for each phase. Next, from this intuitive analysis, we set control objective for each phase and propose control strategy to achieve each control objective which we set previously. In Section IV, we show continuous rolling motion by numerical simulation result. Finally in Section V, we conclude this paper.

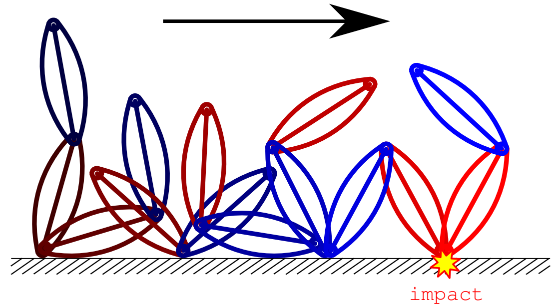

Fig. 1. rolling motion with impact

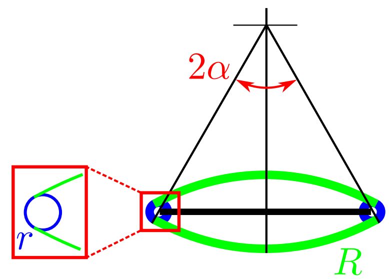

Fig. 2. rounded link

II. Model of the Acrobot with rounded links

A. Robot model

The rounded link of the Acrobot is shown in Fig. 2. As physical parameters, a radius of the tip of the link is r, a radius of the sidepiece of the link is R, and an angle of link's side arc is 2α.

The model of the Acrobot to realize rolling motion differs with contact point between the ground, and it can be divided into five models as follows.

- model-1 (Fig. 3)
  the model during the arc of the tip of link1 contacts with ground.
- model-2 (Fig. 4)
  the model during the arc of the sidepiece of link1 contacts with ground.
- model-3 (Fig. 5)
  the model during the arc between link1 and link2 contacts with ground.
- model-4 (Fig. 6)
  the model during the arc of the sidepiece of link2 contacts with ground.
- model-5 (Fig. 7)
  the model during the arc of the tip of link2 contacts with ground.

978-1-4244-3124-3/08/$25.00 ©2008 IEEE

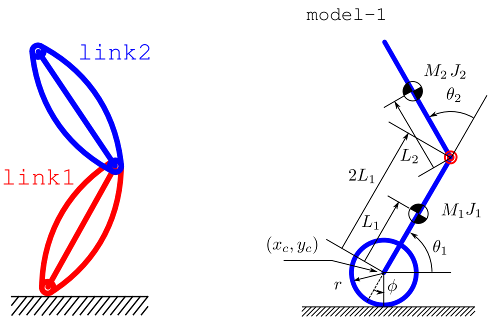

Fig. 3. model-1

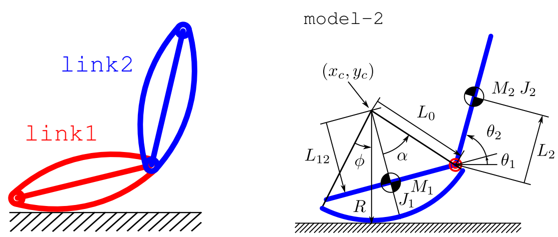

Fig. 4. model-2

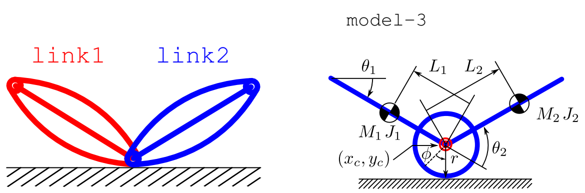

Fig. 5. model-3

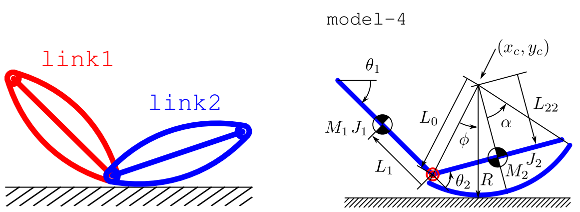

Fig. 6. model-4

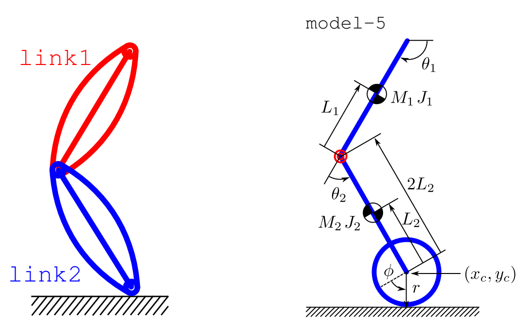

Fig. 7. model-5

θ_1 shows the absolute angle of link1 and θ_2 shows the relative angle of link2. (x_c, y_c) show rotational center of rolling motion. Physical parameters are listed in TABLE I. By geometric relation, rolling angle ϕ is defined as TABLE II.

B. Equation of motion

By Lagrange's method, an equation of motion for each model is derived in the same form as follows.

$$M_f(q_f)\ddot{q}_f + C_f(\dot{q}_f, q_f) + G(q_f) = E_f u + J_c^{\mathrm{T}}\lambda_c \qquad (1)$$

TABLE I

DEFINITION OF PHYSICAL PARAMETERS

M_1, M_2	:	mass of each link
$2L_1$, $2L_2$	:	length of each link (gravity point is at center of the link)
J_1, J_2	:	moment of inertia of each link
L_0	:	length from the rotational center of rolling motion to joint between link1 and link2
L_{12}, L_{22}	:	length from the rotational center of rolling motion to COG of each link

TABLE II

DEFINITION OF ROLLING ANGLE ϕ

model-1	:	$\phi = \pi - \alpha - \theta_1$
model-2	:	$\phi = \alpha - \theta_1$
model-3	:	$\phi = -\alpha - \theta_1$
model-4	:	$\phi = \alpha - (\theta_1 + \theta_2)$
model-5	:	$\phi = -\alpha - (\theta_1 + \theta_2)$

where $q_f = [\theta_1\ \theta_2\ x_c\ y_c]^{\mathrm{T}} \in \mathbb{R}^4$ is a generalized coordinate vector, $M_f \in \mathbb{R}^{4\times4}$ is an inertia matrix, $C_f \in \mathbb{R}^4$ is a Coriolis and centrifugal force, $G_f \in \mathbb{R}^4$ is a gravity term, $E_f = [0\ 1\ 0\ 0]^{\mathrm{T}} \in \mathbb{R}^4$ is an input coefficient vector, and $u \in \mathbb{R}$ is torque input which works at the joint between link1 and link2. M_f, C_f and G_f are different in each model. The rolling constraint of each model is shown as follows.

$$N_c(q_f) = \begin{bmatrix} x_c - a\phi \\ y_c - a \end{bmatrix} = 0 \qquad (2)$$

where

$$a = \begin{cases} r & (\mathrm{model} - 1, 3, 5) \\ R & (\mathrm{model} - 2, 4) \end{cases} \qquad (3)$$

Consequently, the Jacobian $J_c \in \mathbb{R}^{2\times4}$ and constraint force $\lambda_c \in \mathbb{R}^2$ are calculated as follows.

$$J_c = \frac{\partial N}{\partial q_f} = \left[\begin{array}{cc|cc} * & * & 1 & 0 \\ 0 & 0 & 0 & 1 \end{array}\right] = \left[\begin{array}{c|c} J_1 & J_2 \end{array}\right] \qquad (4)$$

$$\lambda_c = (J_c M_f^{-1} J_c^{\mathrm{T}}) \left\{ J_c M_f^{-1}(C_f + G_f - E_f u) + \dot{J}_c \dot{q}_f \right\} \qquad (5)$$

It is known that the equation of motion (1) can be decomposed into a reduced equation of motion by removing the constraint. The reduced equation of motion is represented as follows.

$$M_c(q_c)\ddot{q}_c + C_c(\dot{q}_c, q_c) + G(q_c) = E_c u \qquad (6)$$

where

$$q_c = \begin{bmatrix} \theta_1 \\ \theta_2 \end{bmatrix} \qquad (7)$$

$$J = \begin{bmatrix} I_2 \\ -J_1 \end{bmatrix} \qquad (8)$$

$$M_c(q_c) = J^{\mathrm{T}} M_f J \in \mathbb{R}^{2\times2} \qquad (9)$$

$$C_c(\dot{q}_c, q_c) = J^{\mathrm{T}}(C_f(q, \dot{q}) + \dot{J}\dot{q}_1) \in \mathbb{R}^2 \qquad (10)$$

$$G_c(q_c) = J^{\mathrm{T}} G_f(q) \in \mathbb{R}^2 \qquad (11)$$

$$E_c = J^{\mathrm{T}} E_f \in \mathbb{R}^2 \qquad (12)$$

Finally a state equation with the state $x = [q_c^{\mathrm{T}}\ \dot{q}_c^{\mathrm{T}}]^{\mathrm{T}}$ is derived as follows.

$$\begin{aligned}\dot{x} &= \begin{bmatrix} \dot{q}_c \\ -M_c^{-1}(C_c + G_c) \end{bmatrix} + \begin{bmatrix} 0 \\ M_c^{-1}E_c \end{bmatrix} u \\ &= f(x) + g(x)u\end{aligned} \tag{13}$$

C. Impact model

To realize rolling motion like Fig. 1, we need to model the impact between the Acrobot against the ground.

We assume that a collision of the robot and the ground is perfectly inelastic. At the instant of impacting against the ground, constrained impulse λ_I occurs. Since a variation of both state and input is very small, it can be ignored as compared with λ_I. Therefore, the equation of motion at the instant of impact is represented as follows.

$$\begin{aligned} M_f(\dot{q}_{f+} - \dot{q}_{f-}) &= J_I^T(q_f)\lambda_I \\ J_I(q_f)\dot{q}_{f+} &= 0 \end{aligned} \tag{14}$$

where, $\dot{q}_{f+}$ and $\dot{q}_{f-}$ are the generalized velocity of immediately after and before impact respectively. Then the generalized velocity immediately after impact and the constraint force are derived from (14) as follows.

$$\dot{q}_{f+} = \dot{q}_{f-} - M_f^{-1}J_I^T\lambda_I \tag{15}$$

$$\lambda_I = (J_I M_f^{-1} J_I^T)^{-1} J_I \dot{q}_{f-} \tag{16}$$

When the link1 impacts against the ground, constraint N_I and its Jacobian J_I are represented as follows.

$$\begin{aligned} N_I(q_f) &= \begin{bmatrix} 2L_2\cos(\theta_1+\theta_2+\pi) + 2L_1\cos(\theta_1+\pi) + x_c \\ 2L_2\sin(\theta_1+\theta_2+\pi) + 2L_1\sin(\theta_1+\pi) + y_c \end{bmatrix} \\ &= \text{const.} \end{aligned} \tag{17}$$

$$\begin{aligned} J_I &= \frac{\partial N_I}{\partial q_f} = \begin{bmatrix} J_{I11} & J_{I12} & 1 & 0 \\ J_{I21} & J_{I22} & 0 & 1 \end{bmatrix} \\ J_{I11} &= 2\left\{L_1\sin(\theta_1) + L_2\sin(\theta_1+\theta_2)\right\} \\ J_{I12} &= 2L_2\sin(\theta_1+\theta_2) \\ J_{I21} &= -2\left\{L_1\cos(\theta_1) + L_2\cos(\theta_1+\theta_2)\right\} \\ J_{I22} &= -2L_2\cos(\theta_1+\theta_2) \end{aligned} \tag{18}$$

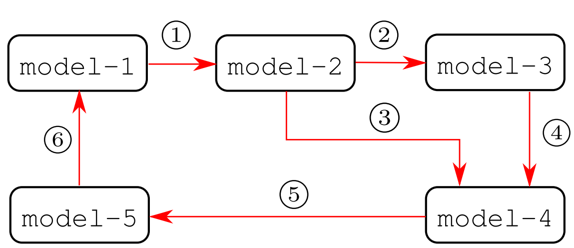

Fig. 8. rolling motion flow

TABLE III

CONDITIONS TO SWITCH MODELS

①	$\phi > \pi - 2\alpha \Leftrightarrow \theta_1 < \alpha$
②	$\phi > 2\alpha \Leftrightarrow \theta_1 < -\alpha,\ \theta_2 > 2\alpha$
③	$\phi > 2\alpha \Leftrightarrow \theta_1 < -\alpha,\ \theta_2 = 2\alpha$
④	$\phi > \delta \Leftrightarrow \theta_1 + \theta_2 < \alpha$
⑤	$\phi > 2\alpha \Leftrightarrow \theta_1 + \theta_2 < -\alpha$
⑥	$2\alpha < \theta_2 < \pi$, link1 contact with ground.

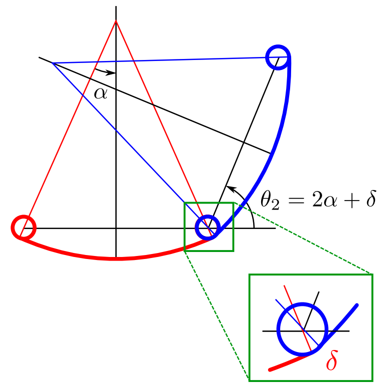

Fig. 9. when $\theta_2 > 2\alpha$

D. Switching of model

The flow of the rolling motion and conditions to switch models are shown as Fig. 8 and TABLE III respectively. Notice that when the model is model-2, to make smooth rolling motion(without impact against ground) of the Acrobot, it is necessary to set θ_2 greater than or equal to 2α (see Fig. 9).

III. Intuitive Analysis and Control of Rolling Motion

Our objective is to make continuous rolling motion of the Acrobot. To achieve this objective, we carry out the procedure to construct the control law as follows. The first, we analyze intuitively the rolling motion where θ_2 is set to a constant value. The second, from this analysis we divide the rolling motion in three phases and construct the control law for each phase.

A. Characteristic of the system

To examine the characteristic of the system, we make a intuitive analysis of the Acrobot's energy while the Acrobot makes the rolling motion which starts from certain standing position with $\theta_2 = \text{const.}$ like Fig. 10. Fig. 11 is time responses of the Acrobot's energy and COG. From Fig. 11 (a), we can see that all energy of the Acrobot is constant during the Acrobot rolls with $\theta_2 = \text{const.}$. Furthermore while the model changes from model-1 to model-3 via model-2, the COG of the Acrobot goes down, and the Acrobot's potential energy decreases and its kinetic energy increases. On the other hand, while the model changes from model-4 to model-5, the COG of the Acrobot goes up, and the Acrobot's kinetic energy decreases and its potential energy increases.

However, when the Acrobot rolls with $\theta_2 = \text{const.}$ and the model becomes model-5, kinetic energy of the Acrobot

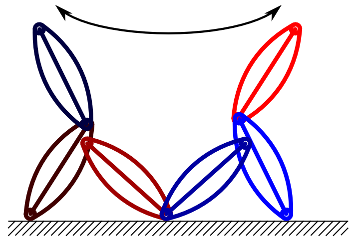

Fig. 10. rolling motion when $\theta_2 = \text{const}$.

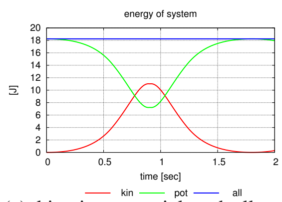

(a) kinetic, potential and all energy of the Acrobot

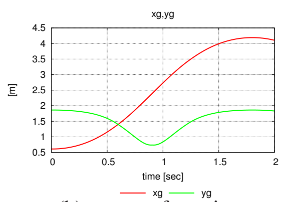

(b) center of gravity

Fig. 11. time response of rolling motion when $\theta_2 = \text{const}$.

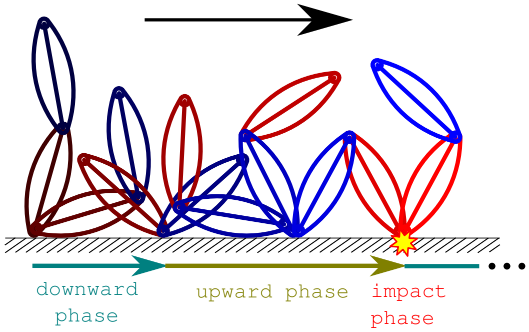

Fig. 12. definition of each phase

decreases and finally becomes 0. Therefore, the Acrobot can't continue the rolling motion to forward direction, and begin to roll to backward direction. As a result of this backward motion the robot repeats the same motion. To make the Acrobot roll continuously to forward direction, we have to keep the Acrobot's kinetic energy high enough.

To devise the control strategy, we divide the rolling motion into three phases as in Fig. 12. Downward phase is the phase while the model changes from model-1 to model-3 via model-2 and the center of the gravity of the Acrobot goes down. Upward phase is the phase while the model changes from model-4 to model-5 and the center of the gravity of the Acrobot goes up. Impact phase is the phase when link1 impacts against the ground when the model is model-5. Why the impact phase is needed becomes clear later.

From the above discussion, the energy flow of downward and upward phase are shown as follows.

- downward phase:
  potential energy $\rightarrow$ kinetic energy
  (Potential energy of the Acrobot is converted into its kinetic energy.)
- upward phase:
  kinetic energy $\rightarrow$ potential energy
  (Kinetic energy of the Acrobot is converted into its potential energy.)

Therefore to keep kinetic energy of the Acrobot high, we need to do as follows.

- downward phase:
  To increase potential energy of the Acrobot for the sake of increasing energy quantity which is transformed into kinetic energy.
- upward phase:
  To keep the Acrobot's potential energy low and increase its kinetic energy.

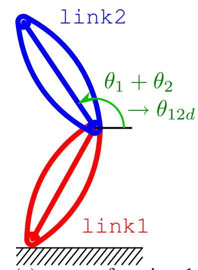

(a) output function 1

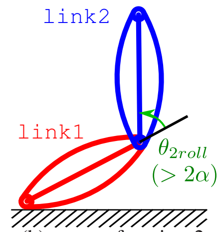

(b) output function 2

Fig. 13. physical interpretation of the output function in downward phase

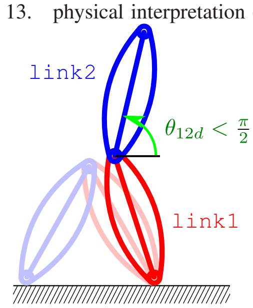

Fig. 14. after impact

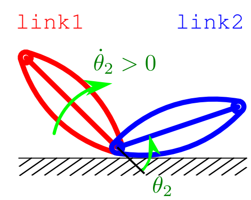

Fig. 15. physical interpretation of the output function in upward phase

B. Downward phase

The control objective in the downward phase is to increase potential energy. Moreover, to make smooth rolling motion of the Acrobot we need to set $\theta_2 \geq 2\alpha$ before the model switches to model-3. Therefore, we need to achieve two different control objective. To realize the first objective, we set the output function as follows.

$$y = \theta_1 + \theta_2 - \theta_{12d} \tag{19}$$

By zeroing this output function, we can control the absolute angle of link2 to desired value θ_{12d} as shown in Fig. 13(a). Moreover, to realize the second objective, if θ_2 becomes θ_{2roll} we change the output function as follows.

$$y = \theta_2 - \theta_{2roll} \tag{20}$$

By zeroing this output function, we can control the angle of link2 to desired value θ_{2roll} as shown in Fig. 13(b). Notice that we use these output functions after the impact phase too.

Next, we discuss how to select the value of θ_{12d} and θ_{2roll}. When $\theta_{12d} = \frac{\pi}{2}$, in other words when the link2 stands vertically, the potential energy becomes maximum because the height of link2's COG becomes maximum. Moreover, considering after impact phase, it is better to set $\theta_{12d} < \frac{\pi}{2}$ because the COG of the Acrobot comes to forward (Fig. 14) and it makes easier to continue the rolling motion of the Acrobot.

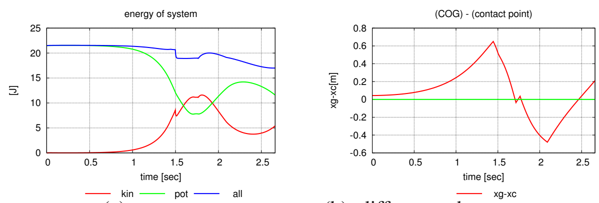

(a) energy

(b) difference between x-coord. of COG and contact point

Fig. 16. when $\dot{\theta}_{2d} > 0$ in upward phase

C. Upward phase

The control objective in the upward phase is to keep potential energy low and increase kinetic energy. To realize this objective, we set the output function as follows.

$$y = \dot{\theta}_2 - \dot{\theta}_{2d} \tag{21}$$

By zeroing this output function, we can control the angular velocity of link2 to desired value $\dot{\theta}_{2d}$ as shown in Fig. 15.

Next, we discuss the value of $\dot{\theta}_{2d}$. When $\dot{\theta}_{2d} > 0$, the COG of the Acrobot goes forward. If the COG is at front of the contact point between the robot and the ground, rolling speed becomes faster and kinetic energy increases as shown in Fig. 16. However, when $\dot{\theta}_{2d} > 0$ the collision between the robot and the ground becomes unavoidable. Therefore, we analyze the impact phase in the next section.

D. Impact phase

Because we assume that the collision between the robot and the ground is perfectly inelastic, the Acrobot loses the kinetic energy at impact phase. We analyze the impact phase in two case. One is the case that the Acrobot impacts with $\dot{\theta}_2 = 0$ and the other is one that the Acrobot impacts with $\dot{\theta}_2 > 0$.

1) Impact with $\dot{\theta}_2 = 0$: We define the kinetic energy ratio of right after to just before impact phase as follows.

$$K_-^+ = \frac{K_+}{K_-} \tag{22}$$

where K_+ is kinetic energy of the Acrobot right after impact phase and K_- is the one just before impact phase. From (16), the relation between $\dot{q}_{f+}$ and $\dot{q}_{f-}$ is shown as follows.

$$\begin{aligned} \dot{q}_{f+} &= A\dot{q}_{f-} \\ A &= I - M_f^{-1} J_I^T (J_I M_f^{-1} J_I^T)^{-1} J_I \end{aligned} \tag{23}$$

Therefore, K_- and K_+ are calculated as follows.

$$K_- = \frac{1}{2}\dot{q}_{f-}^{\mathrm{T}} M_f \dot{q}_{f-} \tag{24}$$

$$K_+ = \frac{1}{2}\left(A\dot{q}_{f-}\right)^{\mathrm{T}} M_f \left(A\dot{q}_{f-}\right) \tag{25}$$

From $\dot{\theta}_{2-} = 0$, (2), (3) and TABLE II, $\dot{q}_{f-}$ is shown as follows.

$$\dot{q}_- = \begin{bmatrix} \dot{\theta}_{1-} \\ \dot{\theta}_{2-} \\ \dot{x}_{c-} \\ \dot{y}_{c-} \end{bmatrix} = \begin{bmatrix} \dot{\theta}_{1-} \\ 0 \\ -r\dot{\theta}_{1-} \\ 0 \end{bmatrix} = \begin{bmatrix} 1 \\ 0 \\ -r \\ 0 \end{bmatrix} \dot{\theta}_{1-} \tag{26}$$

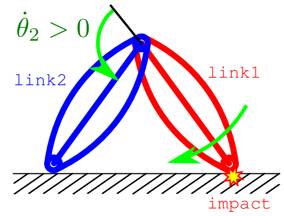

Fig. 17. impact with $\dot{\theta}_2 > 0$

TABLE IV

ENERGY RATIO OF BEFORE TO AFTER IMPACT

$\dot{\theta}_2$ [rad/s]	K_{r-}^+	K_{t-}^+	K_-^+
0.0	$\frac{0.73}{1.19} = 0.614$	$\frac{2.74}{2.88} = 0.949$	$\frac{3.46}{4.07} = 0.852$
0.5	$\frac{0.73}{1.49} = 0.490$	$\frac{2.77}{2.71} = 1.025$	$\frac{3.51}{4.20} = 0.835$
1.0	$\frac{0.73}{1.84} = 0.396$	$\frac{2.80}{2.57} = 1.090$	$\frac{3.53}{4.41} = 0.800$

Letting $b = [1\ 0\ \ -r\ 0]^{\mathrm{T}}$, the energy ratio K_-^+ is shown as follows.

$$K_-^+ = \frac{b^{\mathrm{T}} A^{\mathrm{T}} M_f A b}{b^{\mathrm{T}} M_f b} \tag{27}$$

If θ_2 is fixed, θ_1 has a unique value at impact phase. Therefore, K_-^+ depends only on the value of θ_2 at the moment of impact. When θ_2 is larger K_-^+ becomes close to 1. In other words when the Acrobot is more bent energy loss at impact becomes less.

2) Impact with $\dot{\theta}_2 > 0$: When the Acrobot impacts against the ground with $\dot{\theta}_2 > 0$, the Acrobot kicks the ground as shown in Fig. 17. Therefore there is a possibility that we can increase the kinetic energy of the Acrobot after impact.

The kinetic energy of the Acrobot (28) is divided into rotational energy (29) and translational energy (30)

$$K = K_r + K_t \tag{28}$$

$$K_r = \frac{1}{2}J_1\dot{\theta}_1^2 + \frac{1}{2}J_2\left(\dot{\theta}_1 + \dot{\theta}_2\right)^2 \tag{29}$$

$$K_t = \frac{1}{2}M_1 v_1^2 + \frac{1}{2}M_2 v_2^2 \tag{30}$$

where v_1 and v_2 are a translational velocity of COG of link1 and link2 respectively. From TABLE IV, where K_{r-}^+ and K_{t-}^+ are rotational and translational kinetic energy ratio of right after to just before impact phase respectively, if $\dot{\theta}_2$ becomes larger K_{r-}^+ and K_-^+ becomes less while K_{t-}^+ and the kinetic energy right after impact become larger. This means that if the rotational speed of link1 becomes quick the kinetic energy right after impact becomes large but the efficiency is down.

Considering the control in upward phase, to impact with $\dot{\theta}_2 = 0$ we need to stop the rotation of link1 in upward phase. But if we stop it, the energy consumption

$$E_{cons} = \int_0^T \left|\dot{\theta}_2 u\right| \mathrm{d}t \tag{31}$$

becomes larger. In other words, the rolling motion as a whole becomes less efficient. Therefore, we make the Acrobot impact with $\dot{\theta}_2 = \dot{\theta}_{2d}$ in this paper.

TABLE V
PHYS. PARAMETERS

M_1	1.0 [kg]
M_2	1.0 [kg]
L_1	0.5 [m]
L_2	0.5 [m]
r	0.1 [m]
R	1.1 [m]
α	30.0 [deg]

TABLE VI
INITIAL VALUE

θ_1	90.0 [deg]
θ_2	-10.0 [deg]
$\dot{\theta}_1$	0.0 [deg/s]
$\dot{\theta}_2$	0.0 [deg/s]

TABLE VII
DESIGN PARAMETERS

θ_{12d}	85.0 [deg]
θ_{2roll}	70.0 [deg]
$\dot{\theta}_{2d}$	1.65 [rad/s]

E. Input for output zeroing

1) Downward phase: Because the relative degree of the output function is 2, the torque input for output zeroing is obtained as follows.

$$u = (L_g L_f h)^{-1}(v - L_f^2 h) \tag{32}$$

where L_* is Lie derivative, $h = y$ and v is a new input. The new input v is derived using LQR control.

2) Upward phase: The torque input to control $\dot{\theta}_2$ to desired value $\dot{\theta}_{2d}$ is obtained as follows.

$$u = \frac{v - f_2(x)}{g_2(x)} \tag{33}$$

where $\ddot{\theta}_2 = f_2(x) + g_2(x)u$ and v is a new input. The new input v is derived as follows.

$$v = k_v(\dot{\theta}_2 - \dot{\theta}_{2d}) \tag{34}$$

IV. Simulation

By using the method stated in previous sections, numerical simulation is carried out. Physical parameters and an initial value for the simulation are shown in TABLE V and TABLE VI respectively. The design parameters are chosen as in TABLE VII considering the condition about constraint force as follows.

$$\lambda_y > 0 \tag{35}$$

where λ_y is vertical constraint force. This is the condition to keep the Acrobot contact with the ground.

From the simulation result in Fig. 18, it turns out that the continuous rolling motion has been performed. Fig. 19 shows snapshots of animation of simulation.

V. Conclusion

In this paper, we dealt with continuous rolling motion control for the Acrobot with collision between the Acrobot and the ground. At first, we modeled the Acrobot composed of rounded links to realize rolling motion. Next, we made an intuitive analysis of the Acrobot's energy while the Acrobot rolls with constant relative angle. From this analysis, we divided the rolling motion into three phases and derived the control strategy for each phase. At last, by using the control strategy which was devised from the previous analysis, we realized continuous rolling motion in numerical simulation.

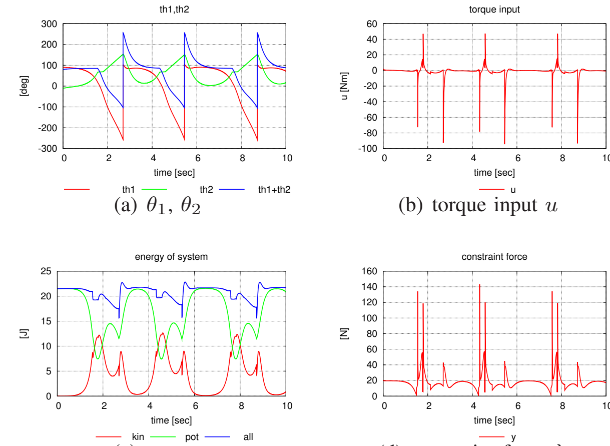

(a) θ_1, θ_2 (b) torque input u

(c) energy (d) constraint force λ_y

Fig. 18. Time response of the simulation of rolling motion

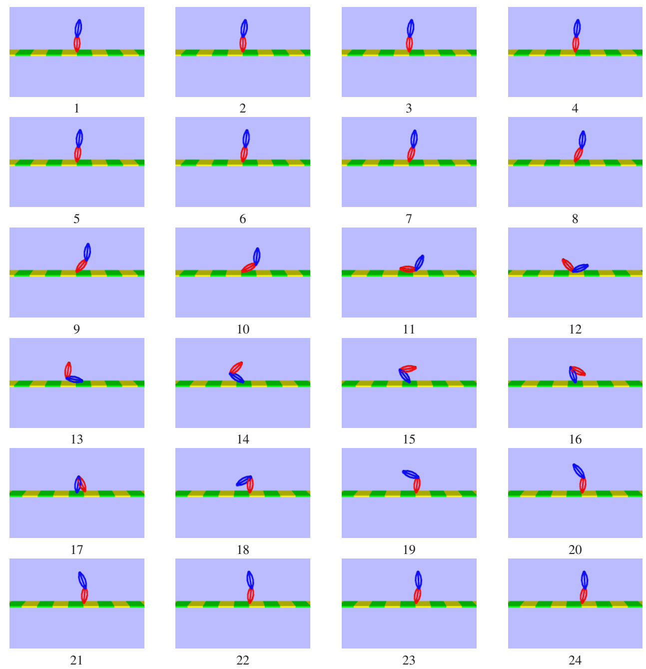

Fig. 19. Rolling motion by simulation

References

[1] Mark W. Spong, Swing Up Control of the Acrobot, *Robotics and Automation, 1994. Proceedings., 1994 IEEE International Conference on*, vol.3, pp 2356-2361.

[2] Ryuichi ANAMI, Masao KANAZAWA, Shigeki NAKAURA and Mitsuji SAMPEI, Swing up Control for Acrobot with Compliance of High Bar Focused on Energy Interaction with Each Component, *Intelligent Robots and Systems, 2007 IEEE/RSJ International Conference on*, 2007, pp 3334-3341.

[3] Masahiro Miyazaki, Mitsuji Sampei, Masanobu Koga and Akiko Takahashi, A Control of underactuated hopping gait systems: Acrobot example,*Decision and Control, 2000. Proceedings of the 39th IEEE Conference on*, 2000, vol.5, pp 4797-4802

[4] Kazuo NAKAKUKI, Kazuo YAMAFUJI and Osamu SHIKATA, Motion Control of A Robot Composed of Three Serial Links with Curved Contour (1st Report, Concept and Dynamic Control of the Robot),*Transactions of the Japan Society of Mechanical Engineers. C*, 1992, vol.58, No.555, pp 3299-3306, (in Japanese)

[5] Kazuo NAKAKUKI, Kazuo YAMAFUJI and Osamu SHIKATA, Motion Control of A Robot Composed of Three Serial Links with Curved Contour (2nd Report, Several Motions of the Robot),*Transactions of the Japan Society of Mechanical Engineers. C*, 1993, vol.59, No.559, pp 850-854, (in Japanese)